

# Structure and physical properties of $\text{Fe}_{59}\text{Mn}_{27}\text{Ni}_7\text{Cr}_3\text{Si}_4$ shape memory alloy

Piotr Lipiński, Dawid Kowalik, Tomasz Kowalski,  
Michał Królicki, Mariusz Hasiak

*Wroclaw University of Science and Technology, Department of Mechanics and Materials Science  
Engineering, 25 Smoluchowskiego St., 50-370 Wrocław, Poland*

**Abstract:** *In this work the authors present the properties of the  $\text{Fe}_{59}\text{Mn}_{27}\text{Ni}_7\text{Cr}_3\text{Si}_4$  (at. %) shape memory alloy. Two different phases were discovered during the XRD analysis and Fe-Mn phase was identified. The hardness of the investigated material in the as-cast state was 194 HV. The nano hardness was 511 HV and Young modulus was determined as 159 GPa. AFM and LFM tests allowed to observe linear arrangement of one phase formed as multiple irregular separations. Shape memory effect was not observed in the temperature range 22 – 600°C.*

**Keywords:** shape memory alloy, microstructure, hardness, AFM, XRD

## 1. Introduction

Fe-Mn-Ni-Cr-Si alloys are ferromagnetic shape memory alloys (FSMAs) [1]. These materials are able to change physical dimensions when energy is delivered. The physical properties of these alloys are extraordinary and unusual [2]. What is more important and unique, the deformation can be fully programmed and adjusted to the appliance. The physical properties are related to the martensite-austenite structure transformation. That is why these alloys are intensively studied and examined. FSMAs are also very common in a commercial application, such as medicine, bioengineering, automotive, which are supported by scientists. Moreover, Fe-based alloys are very often used to eliminate mechanical parts in different devices. They are used as sensors, actuators and in energy-harvesting [3-4] systems.

In this work the authors present the properties of the  $\text{Fe}_{59}\text{Mn}_{27}\text{Ni}_7\text{Cr}_3\text{Si}_4$  (at. %) shape memory alloy. This alloy was chosen due to its low-cost ingredients that allow to apply this alloy in various applications.

## 2. Materials and methods

### 2.1 Materials

The  $\text{Fe}_{59}\text{Mn}_{27}\text{Ni}_7\text{Cr}_3\text{Si}_4$  alloy was created using high purity elements, which were melted in Arc-Melter system. The melting process took place in a protective argon atmosphere. The specimen was remelted five times to get homogeneous alloy. The sample was prepared in tablet form.

## 2.2 X-Ray diffraction analysis

To identify phases discovered in AFM the authors used XRD. The sample in initial state was cleared and prepared to analysis and then set in the device. The specimen was scanned from 20 to 120  $2\theta$ .

## 2.3 Hardness measurement

The measurement of hardness was the first test that was made. The measurement was performed on the sample in as-cast state and the specimen was set in a special vice. The authors used Vicker's method to define hardness. The indenter was a square-based pyramid and it was pressed into the sample with load of 0.5 kgf. The contact time was set to 10 s. Using optical microscope, the authors measured the diagonals and defined hardness.

## 2.4 Nano hardness measurement

The nano hardness measurement was made to show the hardness of one phase. The sample was supplied with 100 mN load and insertion speed 2000 nm/min. Load and insertion time was 30 seconds with 10 seconds break after reaching the set parameters.

## 2.5 AFM analysis

To determine the topography of the examined  $\text{Fe}_{59}\text{Mn}_{27}\text{Ni}_7\text{Cr}_3\text{Si}_4$  alloy in as-cast state the authors performed AFM tests. Several scanning areas were also chosen to determine roughness and LFM analysis was made to detect the number of existing phases.

# 3. Results and discussion

## 3.1 X-Ray diffraction analysis

The results of the X-Ray measurement were shown in Fig. 1. There are several peaks visible that match to different phases.

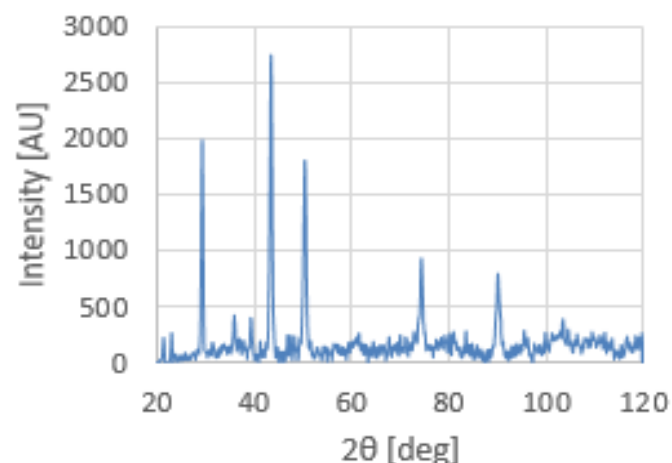


Fig. 1. X-Ray diffraction pattern of the  $\text{Fe}_{59}\text{Mn}_{27}\text{Ni}_7\text{Cr}_3\text{Si}_4$  alloy

Thanks to AFM results the authors predicted that there are at least two phases in the sample. This conclusion was compatible with [5]. However, the authors were able to match only one of

them. The matched phase was Fe-Mn. The reference chart of the Fe-Mn phase was showed in Fig. 2.

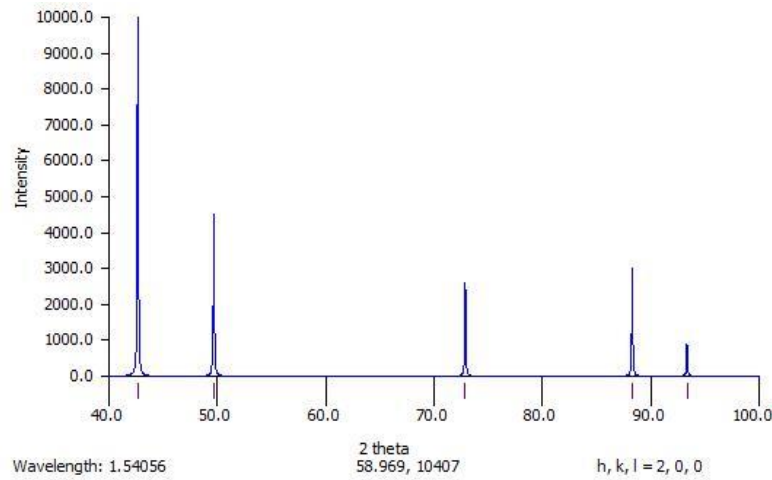


Fig. 2. Reference X-Ray pattern for Fe-Mn phase

The reason why there was only one phase discovered may be the volume of the phases. Probably the Fe-Mn phase had the largest share in the volume of the specimen. The other phase had smaller volume share and it was not discovered in XRD analysis.

### 3.2 Hardness measurement

There were 100 imprints made in the specimen. The imprints are shown in Fig 3.

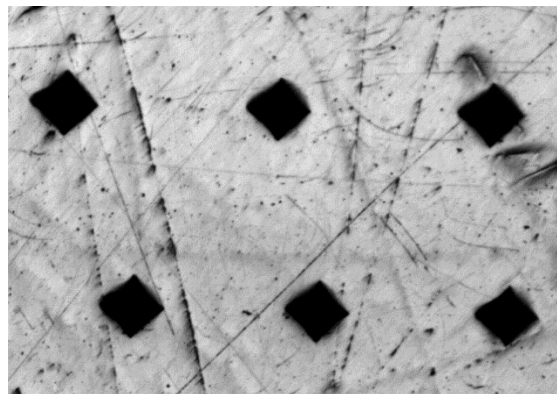


Fig. 3 Multiple imprints made during hardness measurements for the  $\text{Fe}_{59}\text{Mn}_{27}\text{Ni}_7\text{Cr}_3\text{Si}_4$  alloy, (under magnification 10000x)

Based on statistics chart (Fig. 4) and XRD analysis the authors were sure that there is high probability the specimen had more than one phase. Most of the results were between 180 and 210 HV. Local hardness increase could be observed around 183 HV, 195 HV and 205 HV. Based on the results the authors defined hardness of the  $\text{Fe}_{59}\text{Mn}_{27}\text{Ni}_7\text{Cr}_3\text{Si}_4$  alloy as 195 HV. In work [5] the hardness was 315 HV. However, the sample described in [5] was heat treated before the hardness measurement was made.

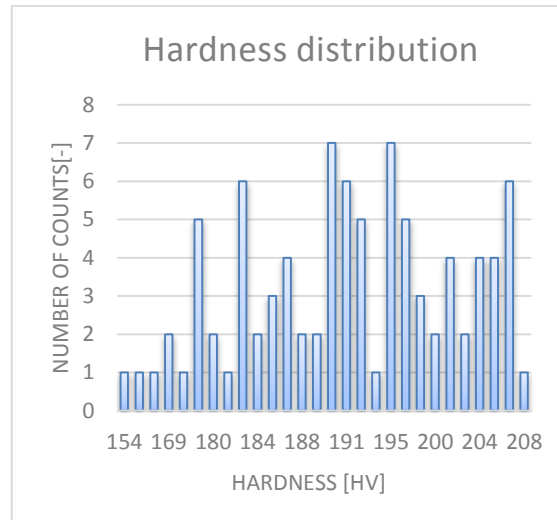


Fig. 4 Distribution of hardness for 100 imprints made in the  $\text{Fe}_{59}\text{Mn}_{27}\text{Ni}_7\text{Cr}_3\text{Si}_4$  alloy

### 3.3 Nano hardness measurement

The imprint made during the measurement of nano hardness is shown in Fig. 5. In Fig. 5 are also presented multiple separations. However, these separations were too small compared to imprint and they were impossible to measure.

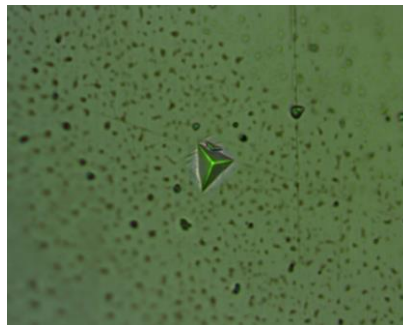


Fig. 5 Imprint made in the  $\text{Fe}_{59}\text{Mn}_{27}\text{Ni}_7\text{Cr}_3\text{Si}_4$  alloy during nano hardness measurement

Except the measurement of nano hardness the authors also defined the strain energy and Young modulus. Young modulus for examined alloy was 159 GPa. The strain energy results are shown in table 1.

Tab. 1 Strain energy for the  $\text{Fe}_{59}\text{Mn}_{27}\text{Ni}_7\text{Cr}_3\text{Si}_4$  alloy during the measurement of nano hardness

Type of deformation	Energy [pJ]
Total energy of strain	34922
Energy of plastic strain	26705
Energy of elastic strain	8217

The strain energy is shown in Fig. 6. The area between 1. – 2. – 3. is the total energy of strain. The area between 1. – 2. – 4. is the energy of plastic strain and between 2. – 3. – 4. is the energy of elastic strain. The result of the measurement of nano hardness was 511 Vickers.

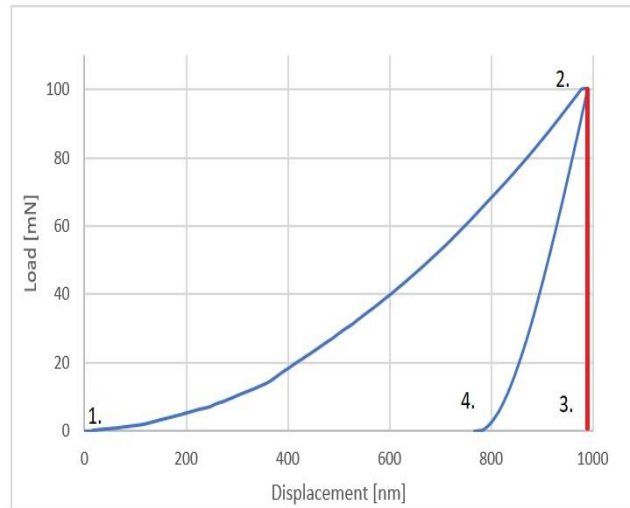


Fig. 6 Load-displacement curve for the  $Fe_{59}Mn_{27}Ni_7Cr_3Si_4$  alloy

### 3.4 AFM analysis

Areas scanned in AFM are shown in Fig. 7 and Fig. 8.

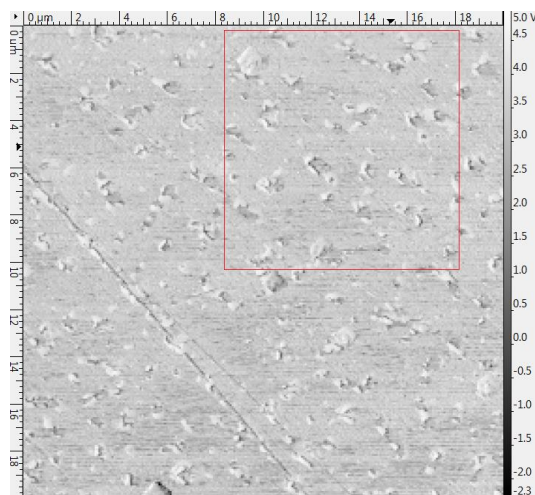


Fig. 7 Topography of the  $Fe_{59}Mn_{27}Ni_7Cr_3Si_4$  alloy with marked area of Fig. 8, scanning area:  $20 \times 20 \mu m$

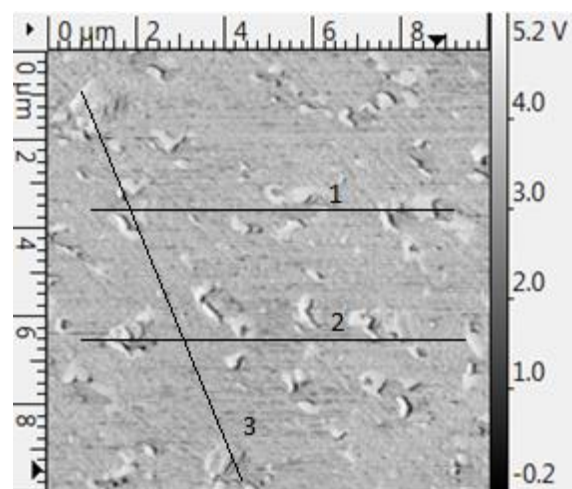


Fig. 8 Topography of the  $Fe_{59}Mn_{27}Ni_7Cr_3Si_4$  alloy with paths for the measurement of roughness, scanning area:  $10 \times 10 \mu m$

Based on previous tests as well as Fig. 7 and Fig. 8 the presence of two different phases can be confirmed. In Fig. 7 second phase is visible as multiple separations.

The roughness was analyzed along selected paths and for the whole area. The paths are shown in Fig. 8. The results for selected paths were compiled in table 2.

Tab. 2 The results for the measurement of roughness for each path

Line	1	2	3
Roughness average Ra	2.97	5.12	2.99

The topography of the selected surface was shown in Fig. 9.

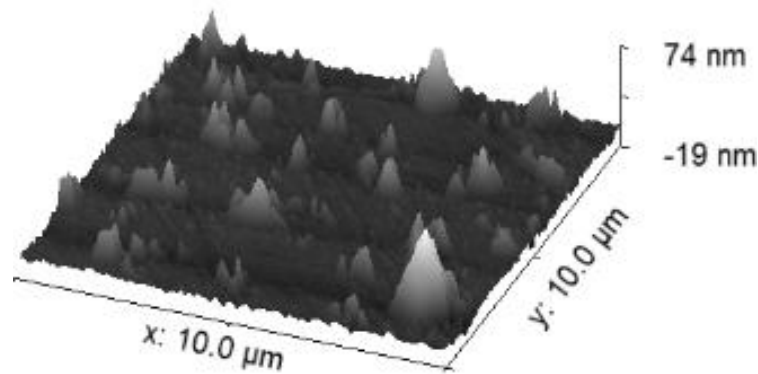


Fig. 9 Topography of the  $\text{Fe}_{59}\text{Mn}_{27}\text{Ni}_7\text{Cr}_3\text{Si}_4$  alloy

Bright spots visible in Fig. 8 were matched to peaks visible in Fig. 9. The pictures proved that there were at least two phases in examined sample. The second phase is shaped in the form of grains surrounded by other phases. The grains stick over the surface what is visible in Fig. 9.

For further analysis of the phases noticed in the studied  $\text{Fe}_{59}\text{Mn}_{27}\text{Ni}_7\text{Cr}_3\text{Si}_4$  alloy the authors used lateral force microscope. The obtained pictures were shown in Fig. 10 a) and b).

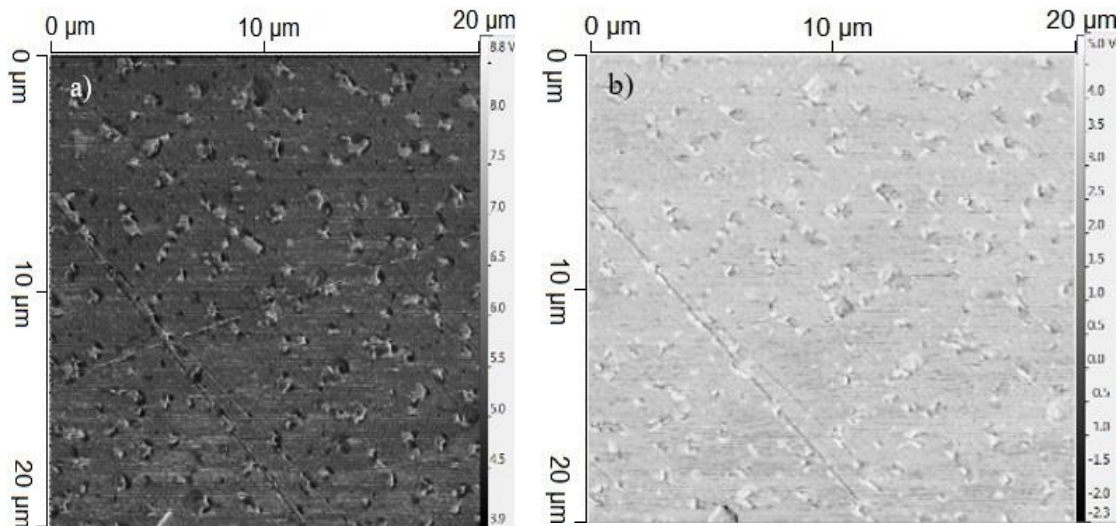


Fig. 10 a), b) Pictures of the  $\text{Fe}_{59}\text{Mn}_{27}\text{Ni}_7\text{Cr}_3\text{Si}_4$  alloy obtained from lateral force microscope, two different phases are visible; scanning area:  $20 \times 20 \mu\text{m}$ .

LFM pictures proved that the first phase is the main phase in the specimen. The main phase has the largest volume in the specimen and creates the main structure. The second phase is in the form of grains showed in Fig. 8 and Fig. 9. This phase is formed with small grains that have specific direction. Linear arrangement is observed for the second phase.

#### 4. Conclusions

Performed tests showed that there was possibility for several phases to exist. The total energy of strain was 34922.31 pJ. The energy of plastic strain was 26704.97 pJ and the energy of resilient strain was 8217.34 pJ. It was impossible to measure hardness of a single phase due to the size of separations. AFM allowed to determine the presence of at least two different phases. Linear

arrangement of one phase was also noticed. The only phase that was identified in XRD was Fe-Mn phase. There were several peaks that weren't matched to reference pattern and they belonged to other unidentified phase. To define other phase correctly further analysis is required. DSC test was made however the shape memory effect was not observed in the temperature range 22 – 600°C. Probably the effect existed in lower temperature than 22°C but it was impossible to get lower values.

## References

- [1] Wen Y.H, Li N., Xiong L.R., Composition design principles for Fe–Mn–Si–Cr–Ni based alloys with better shape memory effect and higher recovery stress, *Materials Science and Engineering*, 2005, Volume 407, Issues 1-2, p. 31-35,
- [2] Faran E., Shilo D., Ferromagnetic shape memory alloys — challenges, applications, and experimental characterization, *Experimental Techniques*, 2016, Volume 40, Issue 3, p. 1-3,
- [3] Besseghini S., Chernenko V.A., Ferromagnetic shape memory alloys: scientific and applied aspects, *La Metallurgia Italiana*, 2007, Issue 11-12, p. 1,
- [4] Barman S.R., Ferromagnetic shape memory alloys, *77th Annual Meeting of Indian Academy of Sciences*, 2011,
- [5] A. Baruj, R. Bolmaro, A.V. Drucker, V. Fuster, J. Malarria, Characterization of phases in a Fe-Mn-Si-Cr-Ni shape memory alloy processed by different thermomechanical methods, *Materials Characterization*, 2015, Volume 109, p. 1-9.